

Structural phases of Fe₄N under pressure

Team 11

(Dated: December 6, 2020)

Abstract We study the structural instability of γ' -Fe₄N as a function of hydrostatic pressure using first principles calculations. At 0 and 10 GPa, we find that the structure is stabilized in the Pm-3m and P2/m symmetry respectively. At 30 GPa, we find several candidates for the structure of Fe₄N which are close in energy.

I. INTRODUCTION

A recently published study on γ' -Fe₄N suggests that several structural instabilities exist as a function of external pressure [1]. At 10 and 30 GPa, the frequency of the phonon near the M and the X point of the Brillouin zone becomes negative respectively. To investigate potential structural phase transitions at these pressures, we perform first principles calculations of the undistorted Pm-3m and the symmetry-lowered P2/m structures of Fe₄N. Then we distort the Pm-3m structure along specific normal mode directions using ISODISTORT [2] and search for candidate structures that are stable at a pressure of 30 GPa.

II. METHODS

Our calculations are carried out using QUANTUM ESPRESSO code [3] with the generalized gradient approximation in the Perdew-Burke-Ernzerhof (PBE) scheme and the projector augmented wave (PAW) method. To determine the appropriate settings for the DFT calculation, we perform k-mesh convergence tests, plane wave cutoff energy (ecutwfc) convergence tests, and charge density cutoff energy (ecutrho) tests on the Pm-3m lattice structure reported in Cheng *et al.* [1] (see Table I). The results of the convergence tests are summarized in Table II, III and IV. We find that a k-mesh of $11 \times 11 \times 11$, ecutwfc = 141 Ry and ecutrho = 564 Ry give a hydrostatic pressure within 1 kbar from the converged hydrostatic pressure. For structural relaxation, we use the Broyden-Fletcher-Goldfarb-Shanno (BFGS) algorithm until forces and stresses are less than 0.001 Ry/Bohr and 0.5 kbar. We use these settings for all the calculations performed for this report.

III. RESULTS

A. Pm-3m structure

Using the lattice parameters of the Pm-3m structure reported in [1] (Table I) we calculate the total energy per atom of γ' -Fe₄N under a uniform volume change using the self-consistent field (scf) method. As the lattice constant a is the only free parameter to vary for the cubic structure, for a given volume the scf calculation gives the

minimal (optimized) total energy. The total energy per atom versus volume per atom is shown in Fig. 1. The Birch-Murnaghan fit is performed over volume changes of -2%, -1%, 0, 1%, 2% and is also shown in Fig. 1. From the fit, we find that the equilibrium volume per atom at 0 GPa is 10.92 \AA^3 , corresponding to a lattice parameter of $a = 3.7937 \text{ \AA}$. The bulk modulus is found to be 188.8 GPa. From the Birch-Murnaghan fit, we derive the hydrostatic pressure ($P = -\partial E / \partial V$) needed to realize the volume change. This is also shown in Fig. 1 as the dashed line. From the P(V) curve, we find that when applying a pressure of 10 GPa, the volume per atom reduces to 10.375 \AA^3 , representing a 5% reduction in volume. This is smaller than the 7% reduction in volume at the same pressure reported in [1]. This could be the result of different pseudopotentials used in the two studies. Our data show that when the volume is reduced by 14%, the pressure obtained from scf calculation is ~ 30 GPa. This differs from the P(V) curve because the Birch-Murnaghan fit is only accurate for $\pm 10\%$ volume change.

B. P2/m structure

Using the lattice parameters of the P2/m structure reported in [1], we perform full structural relaxation at 0 GPa and 10 GPa external pressures. The fully relaxed volume per atom at 10 GPa is found to be 10.239 \AA^3 , which is less than the volume of the Pm-3m structure at 10 GPa. The relaxed lattice parameters and atomic positions at the two pressures are shown in Table I. To obtain the E(V) curve, we adopt two different approaches.

In the first approach, we uniformly expand and compress the equilibrium structure obtained at 0 GPa pressure, and obtain the total energy from scf calculation. We then perform full structural optimization of the uniformly deformed 0 GPa structure under the corresponding pressures determined from the scf calculations. These are shown in Fig. 2 as grey filled circles and black empty circles. We observe that the difference in total energy between the fully relaxed structure and the uniformly deformed structure is very small at small volume changes ($\gtrsim 10 \text{ \AA}^3$). However, at large volume changes ($\lesssim 9.5 \text{ \AA}^3$), the fully relaxed structure has a lower energy than the uniformly deformed structure.

In the second approach, we uniformly expand and compress the equilibrium structure obtained at 10 GPa pres-

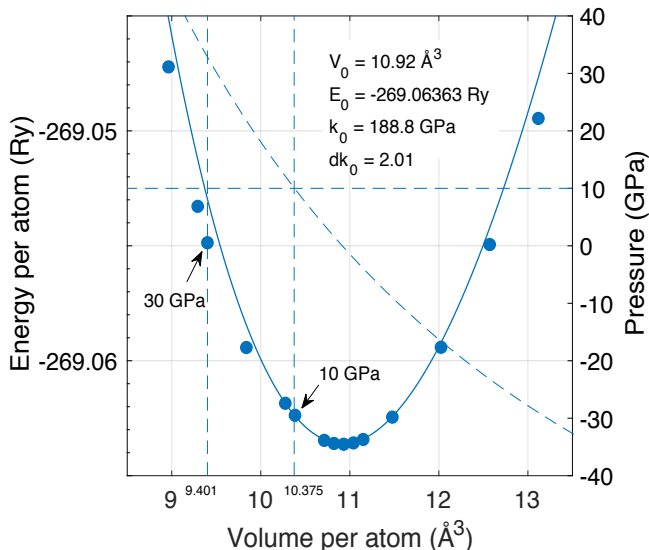


FIG. 1: Total energy per atom versus volume per atom for γ' -Fe₄N in the Pm-3m structure. The volume changes shown here from left to right are -18%, -15%, -14%, -10%, -6%, -5%, -2%, -1%, 0, 1%, 2%, 5%, 10%, 15%, 20%, 25%. The Birch-Murnaghan fit is plotted on top as the blue solid line. The hydrostatic pressure obtained from the Birch-Murnaghan fit is shown as the dotted line. The vertical dashed lines mark the volumes at which a pressure of 10 GPa and 30 GPa is reached.

sure, and obtain the total energy from scf calculation. This approach yields a very similar $E(V)$ curve as the first approach, as shown in Fig. 2 as red empty circles.

In Fig. 3, we show the $E(V)$ curve of the P2/m structure on top of the $E(V)$ curve of the Pm-3m structure. It can be seen that when a pressure of 10 GPa is applied to the Pm-3m structure, the P2/m structure has a lower energy than the Pm-3m structure at the corresponding volume, i.e. there will be a structural phase transition from the Pm-3m structure to the P2/m structure. We also notice that after the structural phase transition, the pressure experienced by the new P2/m structure is slightly less than 10 GPa. The onset of this structural phase transition is determined by the crossing point of the two $E(V)$ curves. According to the two Birch-Murnaghan fits shown in Fig. 3, this happens around 4 GPa in the Pm-3m structure.

C. Structure at 30 GPa

In [1] it is shown the acoustic phonon at $X = (0, 1/2, 0)$ becomes soft at a pressure of 30 GPa. To determine the thermodynamically most stable structure at 30 GPa, we use ISODISTORT[2] to generate distortions of the Pm-3m structure consistent with a soft phonon at X in the Brillouin zone. Five different types of distortion, associated with different types of symmetry breaking, are

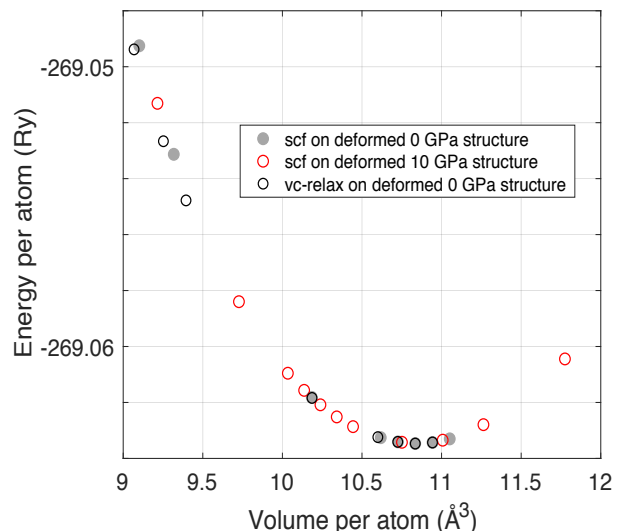


FIG. 2: $E(V)$ for Fe₄N in the P2/m structure. Starting from the fully relaxed structure at 0 GPa, we uniformly deform the structure by a volume change of -16%, -14%, -6%, -2%, -1%, 0, 1%, 2% and obtain the total energy from scf calculation (grey filled circles). We then perform full structural relaxation at several volumes with the corresponding pressures obtained from scf calculations (black empty circles). In a different approach, starting from the fully relaxed structure at 10 GPa, we uniformly deform the structure by a volume change of -10%, -5%, -2%, -1%, 0, 1%, 2%, 5%, 7.5%, 10%, 15% and obtain the total energy from scf calculation (red empty circles).

found: X1+P1 (P4/mmm), X2+P1 (P4/mmm), X5+P1 (Cmcm), X5+P2 (Pmma), X5+C5 (P2/m). In all cases, we set the phonon amplitude to 0.2 and the strains to 0.05 to generate the distorted structures to be used as the input for DFT calculation. We then optimize each of these distorted structures at 0 and 30 GPa. The results are summarized in Table V. At 0 pressure, all of the distorted structures tend to relax to the Pm-3m structure, suggesting that Pm-3m is the stable structure at 0 GPa. At 30 GPa, there is a competition between the different structures as the energy difference between them is less than 0.1 meV per atom. We also relax the P2/m structure discussed in the previous section at 30 GPa. It is found that the P2/m structure at 30 GPa has a higher energy compared to these structures. We provide the fully relaxed lattice parameters and atomic positions of the P4/mmm structure (X2 + P1 distortion) at 30 GPa in Table I.

IV. SUMMARY

We perform first principle calculations on the different structural phases of Fe₄N. We find that the cubic Pm-3m is the stable structure at 0 GPa, the monoclinic

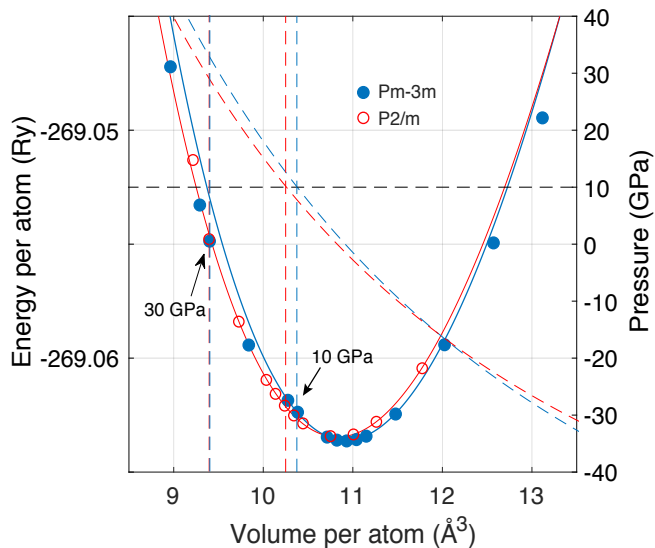


FIG. 3: $E(V)$ for Fe_4N in the Pm-3m structure and the P2/m structure. The total energy per atom versus volume per atom obtained from scf calculation of the uniformly deformed structure is shown for the Pm-3m (blue filled circles) and the P2/m (empty orange circles) structures. The Birch-Murnaghan fits are plotted on top as solid lines. The pressures obtained from the Birch-Murnaghan fits are shown as dashed lines. The horizontal dashed line marks the pressure of 10 GPa. The vertical dashed lines mark the volumes at which a pressure of 10 GPa and 30 GPa is reached in the two structures.

P2/m is the stable structure at 10 GPa. At 30 GPa, we have several candidates for the stable structure, including tetragonal P4/mmm , orthorhombic Cmcm and Pmma , and monoclinic P2/m .

TABLE I: Fe_4N Structures in different symmetries and at different pressures

Space Group	Lattice Parameters	Atomic Position
Pm-3m (0 GPa)	$a = 3.795 \text{ \AA}$	Fe1: 3c (0.5, 0, 0.5) Fe2: 1a (0, 0, 0) N: 1b (0.5, 0.5, 0.5)
P2/m (0 GPa)	$a = 5.3546$ $b = 3.7790$ $c = 5.3546$ $\beta = 90.55^\circ$	Fe1: 1e (0.5, 0.5, 0) Fe2: 2m (0.73019, 0, 0.73013) Fe3: 2m (0.76217, 0, 0.23776) Fe4: 1b (0, 0.5, 0) Fe5: 1f (0, 0.5, 0.5) Fe6: 1h (0.5, 0.5, 0.5) N1: 2n (0.74914, 0.5, 0.74913)
P2/m (10 GPa)	$a = 5.2474$ $b = 3.7188$ $c = 5.2474$ $\beta = 90.58^\circ$	Fe1: 1e (0.5, 0.5, 0) Fe2: 2m (0.72919, 0, 0.72910) Fe3: 2m (0.76421, 0, 0.23571) Fe4: 1b (0, 0.5, 0) Fe5: 1f (0, 0.5, 0.5) Fe6: 1h (0.5, 0.5, 0.5) N1: 2n (0.74884, 0.5, 0.74884)
P4/mmm (30 GPa)	$a = 3.61516$ $b = 3.61516$ $c = 7.22802$	Fe1: (0, 0.5, 0.250028) Fe2: (0.5, 0, 0.249972) Fe3: (0, 0.5, 0.749972) Fe4: (0.5, 0, 0.750028) Fe5: (0.5, 0.5, 0) Fe6: (0.5, 0.5, 0.5) Fe7: (0, 0, 0) Fe8: (0, 0, 0.5) N1: (0.5, 0.5, 0.25) N2: (0.5, 0.5, 0.75)

TABLE II: k-mesh convergence test. P: hydrostatic pressure. E: total energy. $\Delta P(\Delta E)$: difference in P (E) from the converged P (E) from the last row of the table.

k-mesh	P (kbar)	ΔP	E/atom (eV)	$\Delta E/\text{atom}$
$1 \times 1 \times 1$	50.210	91.050	-3660.482	0.240
$3 \times 3 \times 3$	-43.140	2.300	-3660.710	0.012
$5 \times 5 \times 5$	-38.770	2.070	-3660.724	0.002
$7 \times 7 \times 7$	-37.720	3.120	-3660.721	0.001
$9 \times 9 \times 9$	-43.840	-3.000	-3660.722	0.000
$11 \times 11 \times 11$	-41.610	-0.770	-3660.722	0.000
$13 \times 13 \times 13$	-42.03	-1.19	-3660.722	0.000
...
$21 \times 21 \times 21$	-40.84	0.000	-3660.722	0.000

TABLE III: Plane wave cutoff energy convergence test

ecutwfc	ecutrho	P (kbar)	ΔP	$\Delta E/\text{atom}$ (eV)
21	147	-57559.71	57556.94	149.366
41	287	-1830.34	-1827.57	1.882
61	427	-19.51	-16.74	0.125
71	497	-41.61	-38.84	0.032
81	567	-27.35	-24.58	0.012
101	707	-2.8	-0.03	0.007
121	847	-6.7	-3.93	0.002
141	987	-3.41	-0.64	0.002
161	1127	-2.56	0.21	0.001
181	1267	-3.33	-0.56	0.001
...
200	1400	-2.77	0	0.000

TABLE IV: Charge density cutoff energy convergence test

ecutwfc	ecutrho	P (kbar)	ΔP	$\Delta E/\text{atom}$ (eV)
141	282	-2.73	0.560	149.366
141	423	-3.22	0.170	1.882
141	564	-3.36	0.030	0.125
141	705	-3.35	0.040	0.032
141	846	-3.36	0.030	0.012
141	987	-3.41	-0.03	0.007
141	1128	-3.37	-3.93	0.002
...
141	1410	-3.39	0	0.000

TABLE V: Energy for different distortions of γ' -Fe₄N at 30 GPa. In the last row, the energy of the relaxed P2/m structure at 30 GPa is also shown.

Distortion	Energy per atom (Ry)	Energy per atom (Ry)
	at 0 GPa	at 30 GPa
X1 + P1	-269.06354	-269.05489
X2 + P1	-269.06363	-269.05489
X5 + P1	-269.06363	-269.05488
X5 + P2	-269.06363	-269.05488
X5 + C5	-269.06363	-269.05488
P2/m	-269.06347	-269.05478
Pm-3m	-269.06363	

-
- [1] Tai-min Cheng, Guo-liang Yu, Yong Su, Lin Zhu, Lin Li, Spontaneous magnetization-induced phonons stability in γ' -Fe₄N crystalline alloys and high-pressure new phase, *Journal of Magnetism and Magnetic Materials* **451**, 87–95 (2018).
[2] <https://stokes.byu.edu/iso/isodistort.php>
[3] P. Giannozzi, S. Baroni, N. Bonini, M. Calandra, R. Car, C. Cavazzoni, D. Ceresoli, G. L. Chiarotti, M. Cococcioni,

I. Dabo, A. D. Corso, S. de Gironcoli, S. Fabris, G. Fratesi, R. Gebauer, U. Gerstmann, C. Gougoussis, A. Kokalj, M. Lazzeri, L. Martin-Samos, N. Marzari, F. Mauri, R. Mazzarello, S. Paolini, A. Pasquarello, L. Paulatto, C. Sbraccia, S. Scandolo, G. Sclauzero, A. P. Seitsonen, A. Smogunov, P. Umari, and R. M. Wentzcovitch, *J. Phys.: Condens. Matter* **21**, 395502 (2009).